Simulation study of localization of electromagnetic waves in two-dimensional random dipolar systems

Ken Kang-Hsin Wang and Zhen Ye*
Wave Phenomena Laboratory, Department of Physics, National Central University, Chungli 32054, Taiwan
(Received 26 February 2003; revised manuscript received 19 September 2003; published 24 December 2003)

We study the propagation and scattering of electromagnetic waves by random arrays of dipolar cylinders in a uniform medium. A set of self-consistent equations, incorporating all orders of multiple scattering of the electromagnetic waves, is derived from first principles and then solved numerically for electromagnetic fields. For certain ranges of frequencies, spatially localized electromagnetic waves appear in such a simple but realistic disordered system. Dependence of localization on the frequency, radiation damping, and filling factor is shown. The spatial behavior of the total, coherent, and diffusive waves is explored in detail, and found to comply with a physical intuitive picture. A phase diagram characterizing localization is presented, in agreement with previous investigations on other systems.

DOI: 10.1103/PhysRevE.68.066609 PACS number(s): 42.25.Hz, 41.90.+e

I. INTRODUCTION

Over the past two decades, localization of classical waves has been under intensive investigations, leading to a very large body of literature (e.g., Refs. [1–22]). Such a localization phenomenon has been characterized by two levels. One is the weak localization associated with the enhanced backscattering. That is, waves which propagate in the two opposite directions along a loop will obtain the same phase and interfere constructively at the emission site, thus enhancing the backscattering. The second is the strong localization, without confusion often just termed as localization, in which a significant inhibition of transmission appears and the energy is mostly confined spatially in the vicinity of the emission site. While observations of localization of classical waves for one-dimensional systems have been reported [7,9], observation of higher than one dimension remains a subject of much debate [20,22,23].

In a recent paper, a realistic model system has been proposed to study electromagnetic (EM) localization in two-dimensional (2D) random media [24]. This model originated from the previous study of the radiative effects of the electric dipoles embedded in structured cavities [25]. It was shown that EM localization is possible in such a disordered system. When localization occurs, a coherent behavior appears and is revealed as a unique property differentiating localization from either the residual absorption or the attenuation effects. The major advantage of the present system over some previous models such as acoustic waves in bubbly water [18] or water with air-filled cylinders [26] is that it is experimentally available.

With the present paper, we wish to explore further the localization properties of the system outlined in Ref. [24]. We will investigate the dependence of localization behavior on a number of parameters including frequency, filling factor, scattering strength, damping effect, and two different ways of measuring localization. Additionally, the spatial behaviors of the total, coherent, and diffusive wave intensities will be studied, and are shown to comply with a simple physical intuition. We stress that the concepts with regard to the coherent and diffusive waves fully comply with the standard definitions in Refs. [2,27].

II. THE SYSTEM AND THEORETICAL FORMULATION

A. The system

Following Erdogan *et al.* [25], we consider 2D dipoles as an ensemble of harmonically bound charge elements. In this way, each 2D dipole is regarded as a single dipole line, characterized by the charge and dipole moment per unit length. We assume that N parallel dipole lines, aligned along the z axis, are embedded in a uniform dielectric medium and *randomly* located at $\vec{r}_i$ $(i=1,2,\ldots,N)$. The averaged distance between dipoles is d. A stimulating dipole line source is located at $\vec{r}_s$, transmitting a continuous wave of angular frequency ω. By the geometrical symmetry of the system, we only need to consider the z component of the electrical waves.

B. The formulation

Although much of the following materials can be referred to in Ref. [24], we repeat the important parts here for the sake of convenience and completeness.

Upon stimulation, each dipole will radiate EM waves. The radiated waves will then repeatedly interact with the dipoles, forming a process of multiple scattering. The equation of motion for the ith dipole is

$$\frac{d^2}{dt^2}p_i+\omega_{0,i}^2 p_i=\frac{q_i^2}{m_i}E_z(\vec{r}_i)-b_{0,i}\frac{d}{dt}p_i \quad \text{for } i=1,2,\ldots,N, \tag{1}$$

where $\omega_{0,i}$ is the resonance (natural) frequency, p_i, q_i, and m_i are the dipole moment, charge, and effective mass per unit length of the ith dipole, respectively. $E_z(\vec{r}_i)$ is the total electrical field acting on dipole p_i, which includes the radi-

*Electronic address: zhen@phy.ncu.edu.tw ated field from other dipoles and also the direct field from the source. The factor $b_{0,i}$ denotes the damping due to energy loss and radiation, and can be determined by energy conservation. Without energy loss (such as heat), $b_{0,i}$ can be determined from the balance between the radiative and vibrational energies, and is given as [25]

$$b_{0,i}=\frac{q_i^2\omega_{0,i}}{4\epsilon m_i c^2}, \tag{2}$$

with ϵ being the constant permittivity and c the speed of light in the medium separately.

Equation (1) is virtually the same as Eq. (1) in Ref. [25]. The only difference is that in Ref. [25], E_z is the reflected field at the dipole due to the presence of reflecting surrounding structures, while in the present case the field is from the stimulating source and the radiation from all other dipoles.

The transmitted electrical field from the continuous line source is determined by the Maxwell equations [25]

$$\left(\nabla^2-\frac{\partial^2}{c^2\partial t^2}\right)G_0(\vec{r}-\vec{r}_s)=-4\mu_0\omega^2 p_0\pi\delta^{(2)}(\vec{r}-\vec{r}_s)e^{-i\omega t}, \tag{3}$$

where ω is the radiation frequency, and p_0 is the source strength and is set to be unity. The solution of Eq. (3) is clearly

$$G_0(\vec{r}-\vec{r}_s)=(\mu_0\omega^2 p_0)i\pi H_0^{(1)}(k|\vec{r}-\vec{r}_s|)e^{-i\omega t}, \tag{4}$$

with $k=\omega/c$, and $H_0^{(1)}$ being the zeroth-order Hankel function of the first kind.

Similarly, the radiated field from the ith dipole is given by

$$\left(\nabla^2-\frac{\partial^2}{c^2\partial t^2}\right)G_i(\vec{r}-\vec{r}_i)=\mu_0\frac{d^2}{dt^2}p_i\delta^{(2)}(\vec{r}-\vec{r}_i). \tag{5}$$

The field arriving at the ith dipole is composed of the direct field from the source and the radiation from all other dipoles, and thus is given as

$$E_z(\vec{r}_i)=G_0(\vec{r}_i-\vec{r}_s)+\sum_{j=1,j\neq i}^{N}G_j(\vec{r}_i-\vec{r}_j). \tag{6}$$

Substituting Eqs. (4)–(6) into Eq. (1), and writing $p_i=p_i e^{-i\omega t}$, we arrive at

$$(-\omega^2+\omega_{0,i}^2-i\omega b_{0,i})p_i =\frac{q_i^2}{m_i}\left[G_0(\vec{r}_i-\vec{r}_s)+\sum_{j=1,j\neq i}^{N}\frac{\mu_0\omega^2}{4}iH_0^{(1)}(k|\vec{r}_i-\vec{r}_j|)p_j\right]. \tag{7}$$

This set of linear equations can be solved numerically for p_i. After p_i are obtained, the total field at any space point can be readily calculated from

$$E_z(\vec{r})=G_0(\vec{r}-\vec{r}_s)+\sum_{j=1}^{N}G_j(\vec{r}-\vec{r}_j). \tag{8}$$

In the standard approach to wave localization, waves are said to be localized when the square modulus of the field $|E(\vec{r})|^2$, representing the wave energy, is spatially localized after the trivial cylindrically spreading effect is eliminated. Obviously, this is equivalent to saying that the further away is the dipole from the source, the smaller is its oscillation amplitude, expected to follow an exponentially decreasing pattern.

There are several ways to introduce randomness to Eq. (7). For example, the disorder may be introduced by randomly varying such properties of individual dipoles as the charge, the mass, or the two combined. This is the most common way that the disorder is introduced into the tight-binding model for electronic waves [28]. In the present study, the disorder is brought in by the random distribution of the dipoles.

For simplicity yet without losing generality, we assume that all the dipoles are identical and they are randomly distributed within a square area. The source is located at the center (set to be the origin) of this area. For convenience, we make Eq. (7) nondimensional by scaling the frequency by the resonance frequency of a single dipole ω_0. This will lead to two independent nondimensional parameters $b=q^2\mu_0/4m$ and $b_0'=(\omega/\omega_0)(b_0/\omega_0)$. Both parameters may be adjusted in the experiment. For example, the factor b_0 can be modified by coating layered structures around the dipoles [25]. Then Eq. (7) becomes simply

$$(-f^2+1-ib_0')p_i=ibf^2\left[p_0H_0^{(1)}(k|\vec{r}_i-\vec{r}_s|)+\sum_{j=1,j\neq i}^{N}p_jH_0^{(1)}(k|\vec{r}_i-\vec{r}_j|)\right] \tag{9}$$

with $f=\omega/\omega_0$. Equation (9) is self-consistent and can be solved numerically for p_i and then the total field is obtained through Eqs. (3), (5), and (8).

III. THE RESULTS AND DISCUSSION

A. Two numerical measuring scenarios

In the following computation, we will consider two scenarios. They are illustrated in Fig. 1 with the coordinates being shown. In both cases, the sample takes a fixed rectangular shape of which the size may vary. The dipoles, denoted by the small circles, are placed within the rectangle in a complete randomness. The receiver, denoted by the filled black circle, is placed on the x axis.

In case (a), the sample size is fixed. The receiver is placed along x axis to measure the signal at various positions, yielding the result of the transmission signal versus the distance between the source and the receiver, termed as the traveling

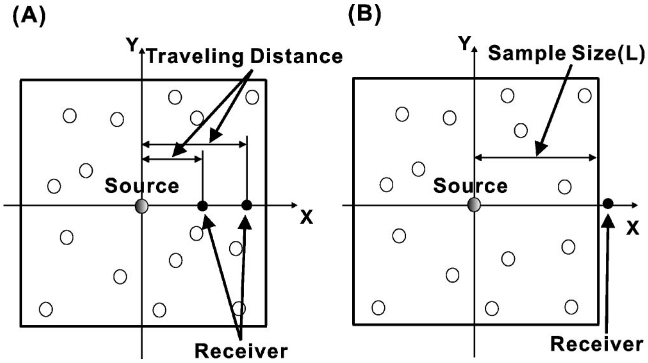

FIG. 1. The conceptual layout of the two measuring methods.

distance in the paper. This scenario complies with the original conjecture of observation of localization [29]. In case (b), the receiver is placed at a very small distance outside the sample. While the sample size varies, this method is to measure the transmission through the sample of various sizes, yielding the result of the transmission signal versus the sample size.

B. General discussion of localization

Before moving to solve Eq. (7) for the phenomenon of localization of EM waves, we discuss some general properties of wave localization.

The coherence in localization. Although some parts of the following discussion have been reported earlier, we repeat here for the sake of convenience and importance. The energy flow of EM waves is $\vec{J}\sim\mathrm{Re}[\vec{E}\times\vec{H}^*]$. By invoking the Maxwell equations to relate the electrical and magnetic fields, we can derive that the time averaged energy flow is

$$\langle\vec{J}\rangle_t\equiv\frac{1}{T}\int_0^T dt\vec{J}\sim\mathrm{Re}[\vec{E}\times\vec{H}^*]=\mathrm{Re}\left[\frac{i}{\omega}\vec{E}\times(\vec{\nabla}\times\vec{E}^*)\right]. \tag{10}$$

Now we write the electrical field as $\vec{E}=\vec{e}_E|\vec{E}|e^{i\theta}$, with $\vec{e}_E$ denoting the direction, $|\vec{E}|$ and θ being the amplitude and the phase, respectively; and taking this into Eq. (10), we arrive at

$$\vec{J}\sim|\vec{E}|^2\vec{e}_E\times(\vec{e}_E\times\vec{\nabla}\theta)=|\vec{E}|^2(\vec{\nabla}\theta)_\perp, \tag{11}$$

where $(\vec{\nabla}\theta)_\perp$ refers to the component of $\vec{\nabla}\theta$ which is perpendicular to the direction of $\vec{E}$. Since in the present 2D system, the electrical field is along the axis of the dipole, therefore by symmetry, $\vec{\nabla}\theta$ is perpendicular to $\vec{E}$. Then Eq. (11) is

$$\vec{J}\sim|\vec{E}|^2\vec{\nabla}\theta. \tag{12}$$

Note that the above equations are exact, and only the constants are omitted in the expression for brevity.

It is clear from Eq. (12) that when θ is constant, at least by spatial domains, while $|\vec{E}|\neq 0$, the flow would come to a stop and the energy will be localized or stored in the space. Therefore in the localized state—someone may call it as a frozen wave, a source can no longer radiate energies. Later we will show that such a phenomenon does appear when waves are localized. As we can see later, all phase vectors defined as $\vec{v}=\vec{e}_x\cos\theta+\vec{e}_y\sin\theta$ tend to point to the same direction. Therefore the current flow tends to zero according to Eq. (12), i.e., no energy radiation. Alternatively, we can write the oscillation of the dipoles as $p_i=|p_i|e^{i\theta_i}$. By studying the square modulus of p_i in the form of $|\vec{r}_i-\vec{r}_s||p_i|^2$, and its phase θ_i, we can also investigate the localization of EM waves. Note here that the factor $|\vec{r}_i-\vec{r}_s|$ is to eliminate the cylindrical spreading effect in 2D as can be seen from the expansion of the Hankel function $|H_0^{(1)}(x)|^2\sim 1/x$. That the phase θ is constant implies that a coherence behavior appears in the system, i.e., the localized state is a phase-coherent state, as previously discussed [26]. It is a unique feature of wave localization, and has also been shown to be related to electronic localization (e.g., Ref. [30]). Here, the coherence refers to that all the oscillations are completely in phase, i.e., θ is constant, at least by domains. This phenomenon is different from the concept of coherent phase in propagating waves.

Spatial behavior of localized waves. Following Ref. [31], a general picture of localized and nonlocalized waves can be described. Without or with little absorption and with no localization, the energy propagation is anticipated as follows. The coherent energy ($\sim|\langle E\rangle|^2$) is decaying due to attenuation by scattering, yielding a steady growth of the incoherent or diffusive energy ($\sim\langle|E|^2\rangle-|\langle E\rangle|^2$). When there is localization, the wave will be trapped within an *e*-folding distance from the penetration. In the nonlocalization case, the diffusive intensity increases steadily as more and more scattering occurs, complying with the Milne diffusion. In the localized state, the diffusion energy increases initially. It will eventually stop growing, followed by a decrease due to the interference of multiple scattering waves. Issues may be raised with respect to whether this apprehended image is supported by actual situations. In the rest, we will inspect this problem. We note that here we discuss only the energy distribution instead of energy flow, since in reality it is the energy which is mostly to be measured. As far as the energy flow is concerned, according to the previous discussion we expect that the flow is zero when localization occurs.

C. Numerical results

Unless otherwise noted, the following parameters are used in the numerical simulation: the nondimensional damping rate $b_0/\omega_0=0.001$ and the interaction coupling $b=0.001$. The filling factor (β) varies from 2.25 to 25; the filling factor is defined as the number of dipoles per unit area. But without notification, the filling factor is taken as 6.25. The number of random configurations for averaging is taken in such a way that the convergency is assured. In the calculation, we scale all lengths by a length D such that $k_0D=1$, and frequency by ω_0. In this way, the frequency always enters as k/k. We find that all the results shown below are only dependent on parameters b, b_0/ω_0, and the ratio ω/ω_0 or equivalently k/k_0. Such a simple scaling property may facilitate designing experiments. In the numerical computation,

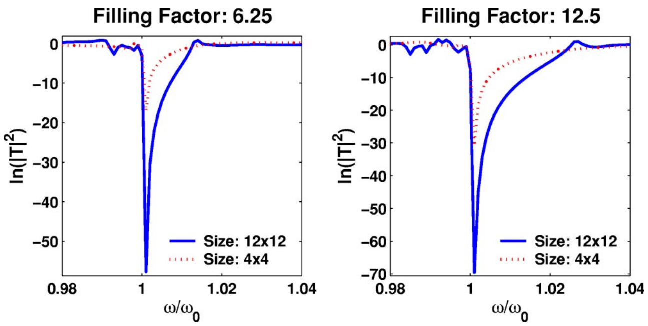

FIG. 2. Transmission vs frequency for two filling factors and two sample sizes.

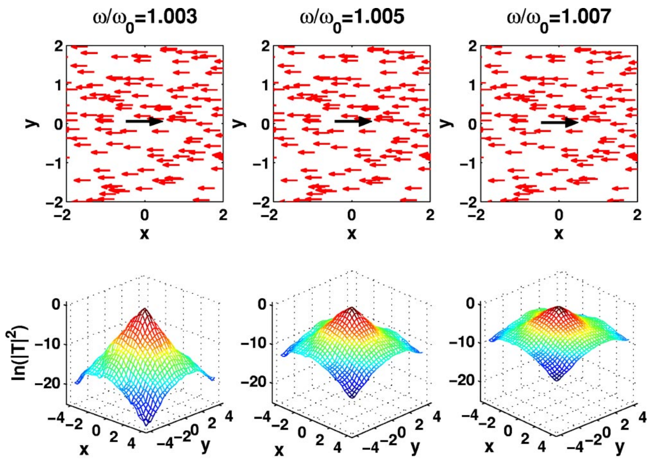

FIG. 3. The phase diagram for the two-dimensional phase vectors defined in the text; the phase of the source is assumed to be zero. Each vector is located at the site of the dipole; thus the locations of the phase vectors also denote the random distribution of the dipoles. Bottom: The spatial distribution of energy ($\sim |T|^2$). Three frequencies are chosen, the sample size is 8×8.

we take $c=1$ for convenience. The total wave at a spatial point is scaled as $T(\vec{r})\equiv E(\vec{r})/E_0(\vec{r})$, with E_0 being the direct wave from the source, so that the trivial geometric spreading effect is naturally removed.

First, we plot the frequency response of the transmission in the scenario (b) of Fig. 1. The results are shown in Fig. 2. Here we see that there is a narrow window within which the transmission is highly inhibited, implying a strong localization effect. It is also clear that when the sample size is increased, the inhibition increases. Comparing the results for the two filling factors, we know that the strong inhibition regime increases with filling factor. In the next computations, we will focus on frequencies within the strong inhibition region.

Now we consider the phase and the spatial distribution of energy of the system. To describe the phase behavior of the system, we assign a unit phase vector $\vec{u}_i = \cos\theta_i \vec{e}_x + \sin\theta_i \vec{e}_y$ to the oscillation phase θ_i of the dipoles. Here $\vec{e}_x$ and $\vec{e}_y$ are unit vectors in the x and y directions, respectively. These phase vectors are represented by a phase diagram in the x-y plane with the phase vector $\vec{u}_i$ being located at the dipole to which the phase θ_i is associated. The results are depicted for three frequencies in Fig. 3.

Here we see clearly that for the three frequencies within the strong inhibition region, the energy is spatially confined near the transmitting source, and, as expected, the energy seems to decrease nearly exponentially along any radial direction. Meanwhile, the system reveals an in-phase phenomenon: nearly all the phase vectors of the dipoles point to the same direction, exactly opposite to the phase vector of the source which is denoted by the black arrow. The picture represented in Fig. 3 fully complies with the general description of the coherence in localization stated above.

We also note from Fig. 3 that near the sample boundary, the phase vectors start to point to different directions. This is because the numerical simulation is carried out for a finite sample size. For a finite system, the energy can leak out at the boundary, resulting in disorientation of the phase vectors. When enlarging the sample size by adding more dipoles while keeping the averaged distance between dipoles fixed, the area showing the phase coherence will increase accordingly.

The results of Fig. 3 are encouraging, as they are a strong indication of localization. In the following, we will further explore the features of localization. In Fig. 4, we compare the transmission results for the two scenarios from Fig. 1. Here it is shown that although there is a slight difference in the transmitted strength, generally speaking the spatial decay features are nearly identical, signified by the match of the decaying slopes indicated in the figure. Though suspected to be true previously, such a match is important, and to the best of our knowledge this is the first that has been ever shown for EM waves. It supports directly that the scenario (b) can also be used to infer localization effects, facilitating measurements of localization; in the original conjecture, it was scenario (a) that has been suggested for discerning localization. In the rest of simulation, we will adopt scenario (b) in Fig. 1.

The bottom panel of Fig. 3 indicates that the level of spatial localization of energy varies for the three frequencies. To quantify the localization in Fig. 3, we plot the total energy as a function of the sample size. The results are presented in Fig. 5. Here, the numerical data are fitted with the least squares method and the fitted curves are shown by the solid lines; the unnoticeable deviation from the lines reflects the fluctuation due to the random distribution. Two ways of averaging are adopted. One is the traditional way in which the

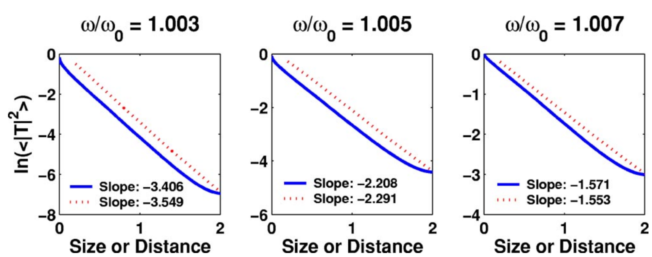

FIG. 4. Comparison of the total transmission at three frequencies for the two scenarios shown in Fig. 1. The x labels ''Distance'' and ''Size'' refer to scenarios (a) and (b), respectively. The solid and dotted lines refer to (a) and (b), respectively.

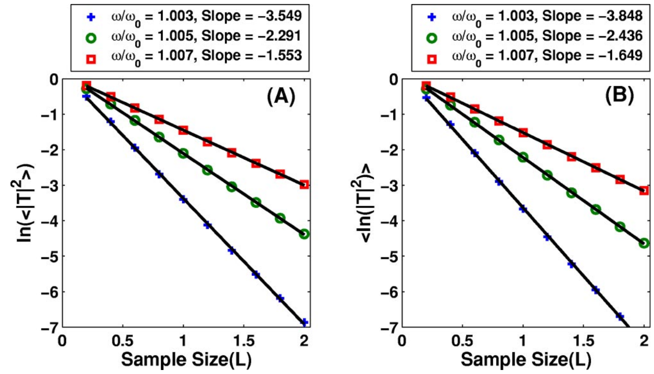

FIG. 5. The transmission vs the sample size for three frequencies. The slopes can be used to estimate the localization length.

logged total transmission is averaged, while the other is to take log of the averaged total energy. These can be referred to from the y-axis labels. It shows that after removing the spreading factor, the data can be fitted by $e^{-r/\xi}$. From the slope of the solid lines, the localization lengths ξ, which are the inverse of the slopes, can be estimated. Here it is shown that the decaying slopes from the two averaging methods are very close, an encouraging fact. It is also indicated by the decrease of the slopes with frequency that the localization effect decreases as the frequency increases.

With the fixed filling factor of 6.25, we have also investigated the spatial variations of the total, coherent, and the diffusive energies for three frequencies discussed. The results are presented in Fig. 6. Here we see that the results are in accordance with the above general consideration of localization. That is, due to scattering and localization, the coherent waves decrease with the sample size. The diffusive wave increases initially as more and more scattering occurs, then reaches a peak and starts to decay due to the localization effect. The results show that in the present system, the diffusive portion in the total energy is much smaller than the coherent portion, indicating that the mean free path is very small. When plotted in the log scale, we have found that the total and coherent energies decay exponentially with the distance, while the diffusive energy increases initially, then starts to decay exponentially. It is worth noting that for the three frequencies considered, the total energy does not reveal any behavior similar to the diffusive waves, in contrast to the previous theoretical conjecture [2]. The theory predicts that the total energy would follow the behavior of diffusive waves until the sample size is larger than the localization length. One explanation is that in the present system, the scattering is too significant so that the diffusive portion never dominates. A search for the possible match between the simulation and theory in certain conditions is still undergoing.

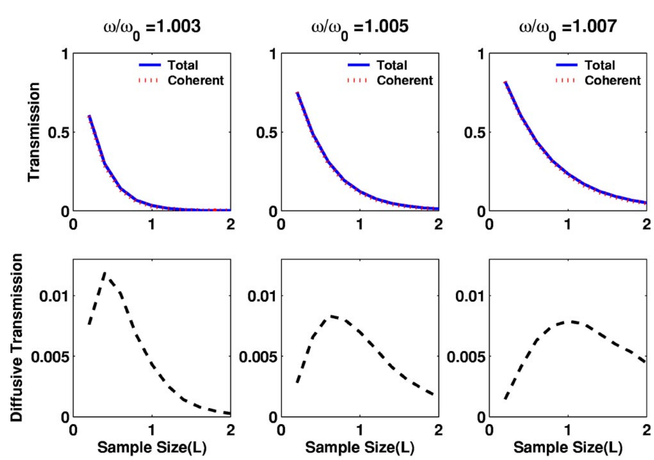

FIG. 6. Behaviors of the total, coherent, and the diffusive energies as a function of sample size in the scenario described in Fig. 1(b).

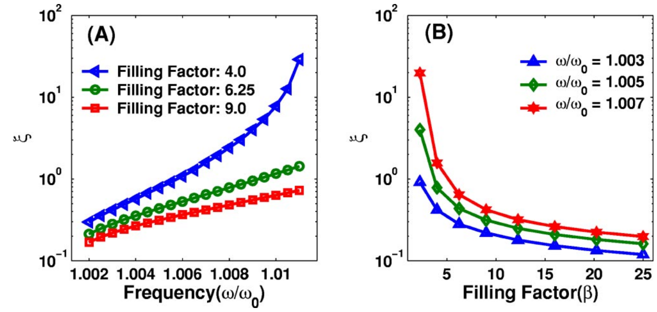

FIG. 7. Localization length as a function of (a) frequency and (b) filling factor. The sample size is 8×8 for (a).

In Fig. 7, we plot the localization length versus frequency and filling factor separately. It is shown that with the fixed filling factor, referring to Fig. 7(a), the localization length increases with frequency within the frequency regime considered. With a fixed frequency, the localization length tends to decrease, meaning increasing localization effects, as the filling factor increases.

Figure 8 shows the transmission versus frequency for various coupling constants and damping rates. From this figure, we observe the following.

(1) The increasing coupling strength leads to a wider strong inhibition region, but shallower localization valley.

(2) When increasing the coupling strength, a prominent resonance peak appears below the natural frequency ω_0, and the peak moves toward lower frequencies as the strength

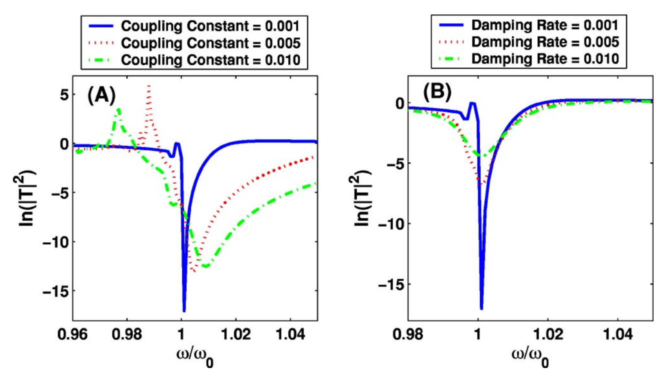

FIG. 8. Transmission vs frequency for various coupling strengths and damping factors: (a) various coupling strengths with damping rate 0.001; (b) various damping rates with coupling constant 0.001. The sample size is 4×4.

increases, a feature that also appears in the acoustic system [18].

(3) Generally speaking, the increasing damping rate degrades the localization level, and tends to abolish the resonance peak. Also it seems to widen the strong localization region at the lower frequency side.

IV. SUMMARY

In this paper, the localization features in a simple electromagnetic system are investigated in detail. Some general properties of the localization phenomenon are elaborated. For certain ranges of frequencies, strongly localized electromagnetic waves have been observed in such a simple but realistic disordered system. It is shown that the localization depends on a number of parameters including frequency, filling factor, and damping rate. The spatial behavior of the total, coherent, and diffusive waves is also explored, and found to comply with a physical intuitive picture. A phase diagram characterizing localization is presented, in agreement with previous investigations on other systems [26].

ACKNOWLEDGMENTS

This work was supported by the National Science Council of Republic of China and Department of Physics at NCU.

[1] S. John, Phys. Today **44**(5), 52 (1991).

[2] P. Sheng, *Introduction to Wave Scattering, Localization, and Mesoscopic Phenomena* (Academic Press, New York, 1995).

[3] A. Lagendijk and B.A. van Tiggelen, Phys. Rep. **270**, 143 (1996).

[4] B. A. van Tiggelen, *Diffuse Waves in Compex Media* (Kluwer Academic, Netherlands, 1999).

[5] M.C.W. van Rossum and Th.M. Nieuwenhuizen, Rev. Mod. Phys. **71**, 313 (1999).

[6] M. Janssen, *Fluctuations and Localization* (World Scientific, Singapore, 2001), and references therein.

[7] C.H. Hodges and J. Woodhouse, J. Acoust. Soc. Am. **74**, 894 (1983).

[8] T.R. Kirkpatrick, Phys. Rev. B **31**, 5746 (1985).

[9] S. He and J.D. Maynard, Phys. Rev. Lett. **57**, 3171 (1986).

[10] C.A. Condat, J. Acoust. Soc. Am. **83**, 441 (1988).

[11] D. Sornette and B. Souillard, Europhys. Lett. **7**, 269 (1988).

[12] A.Z. Genack and N. Garcia, Phys. Rev. Lett. **66**, 2064 (1991).

[13] R. Dalichaouch, J.P. Armstrong, S. Schultz, P.M. Platzman, and S.L. McCall, Nature (London) **354**, 53 (1991).

[14] S.L. McCall, P.M. Platzman, R. Dalichaouch, D. Smith, and S. Schultz, Phys. Rev. Lett. **67**, 2017 (1991).

[15] M. Rusek and A. Orlowski, Phys. Rev. E **51**, R2763 (1995).

[16] M.M. Sigalas, C.M. Soukoulis, C.-T. Chan, and D. Turner, Phys. Rev. B **53**, 8340 (1996).

[17] A.A. Asatryan *et al.*, Phys. Rev. B **57**, 13 535 (1998).

[18] Z. Ye and A. Alvarez, Phys. Rev. Lett. **80**, 3503 (1998).

[19] B. Gupta and Z. Ye, Phys. Rev. E **67**, 036606 (2003).

[20] D.S. Wiersma, P. Bartolini, A. Lagendijk, and R. Roghini, Nature (London) **390**, 671 (1997).

[21] Y. Kuga and A. Ishimaru, J. Opt. Soc. Am. A **1**, 831 (1984); M. van Albada and A. Lagendijk, Phys. Rev. Lett. **55**, 2692 (1985); P.E. Wolf and G. Maret, *ibid.* **55**, 2696 (1985); A. Tourin *et al.*, *ibid.* **79**, 3637 (1997); M. Torres, J.P. Adrados, and F.R. Montero de Espinosa, Nature (London) **398**, 114 (1999).

[22] A.A. Chabanov, M. Stoytchev, and A.Z. Genack, Nature (London) **404**, 850 (2000).

[23] F. Scheffold, R. Lenke, R. Tweer, and G. Maret, Nature (London) **398**, 206 (1999); D. Wiersma *et al.*, *ibid.* **398**, 207 (1999).

[24] Z. Ye, S. Li, and X. Sun, Phys. Rev. E **66**, 045602(R) (2002).

[25] T. Erdogan, K.G. Sullivan, and D.G. Hall, J. Opt. Soc. Am. B **10**, 391 (1993).

[26] E. Hoskinson and Z. Ye, Phys. Rev. Lett. **83**, 2734 (1999).

[27] A. Ishimaru, *Wave Propagation and Scattering in Random Media* (Academic Press, New York, 1978), Vols. I and II.

[28] R. Zallen, *The Physics of Amorphous Solids* (Wiley, New York, 1983).

[29] P.A. Lee and Ramakrishnan, Rev. Mod. Phys. **57**, 287 (1985).

[30] S.A. Gutvitz, Phys. Rev. Lett. **85**, 812 (2000), and references therein.

[31] Z. Ye, H.-R. Hsu, E. Hoskinson, and A. Alvarez, Chin. J. Phys. (Taipei) **37**, 343 (1999).